Impact of Cs Substitution on the Optoelectronic Properties of $MASnI_3$ Perovskite: A DFT study

Abdelhafid Najim[1*], *Lhouceine* Moulaoui[2], *Omar* Bajjou[3], and *Khalid* Rahmani[4]

[1]Sultan Moulay Slimane University of Beni Mellal, Multidisciplinary Research and Innovation Laboratory, FP Khouribga, BP. 145, 2500 Khouribga, Morocco
[2]LRPSI, Faculty of Polydisciplinary, Sultan Moulay Slimane University, B.P 592, 23000, Beni Mellal-Morocco
[3]Laboratory of Engineering in Chemistry and Physics of Matter (LIPCM), Faculty of Sciences and Technics, Sultan Moulay Slimane University, B.P 523, 23000 Beni Mellal, Morocco
[4]PSES, ERC, Ecole Normale Supérieur, Mohammed V University in Rabat, P. O. Box: BP5118 Takkadoum Rabat-10000, Morocco

Abstract. The electronic structures and optical characteristics of pristine $MASnI_3$ ($MA = CH_3NH_3$) perovskite and cesium (Cs)-substituted $MASnI_3$ were investigated using density functional theory (DFT). The structures were constructed, optimized, and analyzed with the CASTEP code to obtain their band structures and optical properties. This perovskite material is of great interest for next-generation optoelectronic devices. Substituting Cs in $MASnI_3$ perovskite reduces the band gap from 1.051 eV to 0.984 eV and alters the optical response. The incorporation of Cs into the $MASnI_3$ perovskite significantly influences its electronic and optical characteristics, indicating that Cs substitution is a promising strategy for tuning these properties.

Keywords: $MASnI_3$; Cesium; absorption coefficient; CASTEP.

1 Introduction

Recently, organometallic halide perovskites have been employed in the development of solar devices with remarkable efficiency [1]. Future energy demands can be met by harnessing the most abundant and clean energy source available—sunlight—through the widespread commercial application of cost-effective, environmentally friendly, and sustainable energy storage and power conversion technologies. Organic–inorganic perovskite materials have attracted significant attention from both the scientific and industrial communities because of their outstanding optoelectronic properties, such as strong visible-light absorption, an ideal band gap, and high charge-carrier mobility [2]. Organic-inorganic hybrid perovskite materials like $MASnI_3$ exhibit outstanding optical and electrical properties, making them highly suitable for photovoltaic applications such as light-emitting diodes, photodetectors, and solar cells. $MASnI_3$ offers several advantages, including low cost, simple solution processing, and low synthesis temperatures [3]. The direct band gap of $MASnI_3$, a p-type

* Corresponding author: abdelhafid.najim@usms.ma

semiconductor, is approximately 1.3 eV [4]. In lead-free perovskite solar cells, $MASnI_3$ was initially used as the absorbing layer in 2014, achieving a device efficiency of 5.73% [5,6].

Cesium-based materials exhibit excellent optical and electrical properties [7,8]. Their band gap can be readily tuned, making them highly attractive for applications in displays and optoelectronic devices [9,10]. As a result, these materials have attracted considerable attention as promising candidates for such technologies [11]. To improve the overall photovoltaic performance of perovskite materials, substitution or doping of $MASnI_3$ components with other ions has been extensively investigated [12]. To date, chemical substitution at the MA site remains the most widely employed strategy in experimental research on perovskite solar cells. Among the monovalent alkali cations, Cesium (Cs^+) is the most commonly studied as a replacement in the light-absorbing layer, due to its superior thermal stability [13]. For single-junction solar cells, researchers have begun introduced mixed-cation systems such as Cs–MA, Cs–FA (FA = $CH(NH_2)_2$), and Cs–MA–FA to form perovskites. The incorporation of Cs has been shown to effectively reduce trap states and enhance device performance [14,15]. Therefore, this study aims to explore novel perovskite light absorbers. In this study, we present a theoretical investigation of Cs-doped methylammonium tin iodide ($MA_{1-x}Cs_xSnI_3$) perovskites as potential light-absorbing materials [16].

2 Computational Methods

The optoelectronic properties of pristine $MASnI_3$ and cesium-doped $MASnI_3$ structures were investigated using DFT calculations. All computations were performed with the CASTEP code, employing on-the-fly generated (OTFG) ultrasoft pseudopotentials. The Perdew–Burke–Ernzerhof (PBE) functional within the generalized gradient approximation (GGA) was used to calculate the exchange-correlation energy [17]. This functional was selected for its ability to effectively capture the exchange and correlation effects in the electronic structure calculations, providing a good balance between computational efficiency and the accuracy required for modeling complex materials like perovskites [18]. For all computations, a plane-wave energy cutoff of 500 eV was employed to ensure the accuracy and convergence of the results [19,20]. The Brillouin zone was sampled using a 5×5×1 Monkhorst-Pack grid to optimize the geometries of both pristine and Cs-doped $MASnI_3$ structures. The convergence tolerance for geometry optimization was set to 2×10^{-6} eV/atom for the total energy for all structural relaxations [21,22]. Atomic positions were optimized until the forces on each atom were less than 0.04 eV/Å, and atomic displacements were limited to within 0.03 Å. The self-consistent field (SCF) convergence tolerance was also set to 2×10^{-6} eV/atom. Additionally, a maximum stress threshold of 0.1 GPa was used to guarantee accurate and stable optimization results [23,24]. The optimized structures of pristine and Cs-doped $MASnI_3$ are illustrated in Fig. 1.

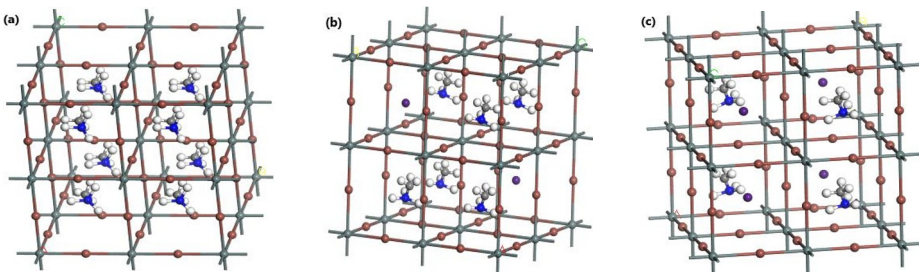

Fig. 1. Crystal structures of (a) $MASnI_3$, (b) $MA_{0.75}Cs_{0.25}SnI_3$, and (c) $MA_{0.5}Cs_{0.5}SnI_3$. The Cs atoms indicated by the purple spheres.

3 Results and discussions

3.1 Electronic structure

The band structures of pristine $MASnI_3$ and Cs-doped $MASnI_3$ materials, calculated along the high-symmetry directions of the Brillouin zone, are shown in Fig. 2. The analysis reveals that these materials exhibit a direct band gap, as both the valence band maximum (VBM) and the conduction band minimum (CBM) are located at the G point of the Brillouin zone. The calculated band gap values for pristine $MASnI_3$, $MA_{0.75}Cs_{0.25}SnI_3$, and $MA_{0.5}Cs_{0.5}SnI_3$ are 1.051 eV, 1.005 eV, and 0.984 eV, respectively [25]. The observed decrease in band gap with increasing cesium concentration reflects the semiconducting nature of these structures. Cs doping effectively narrows the band gap energy, indicating that the modification of electronic states caused by symmetry breaking in the $MASnI_3$ lattice significantly influences its electronic structure. Therefore, both pristine and Cs-doped $MASnI_3$ perovskites can be considered promising semiconductors for photodetector applications.

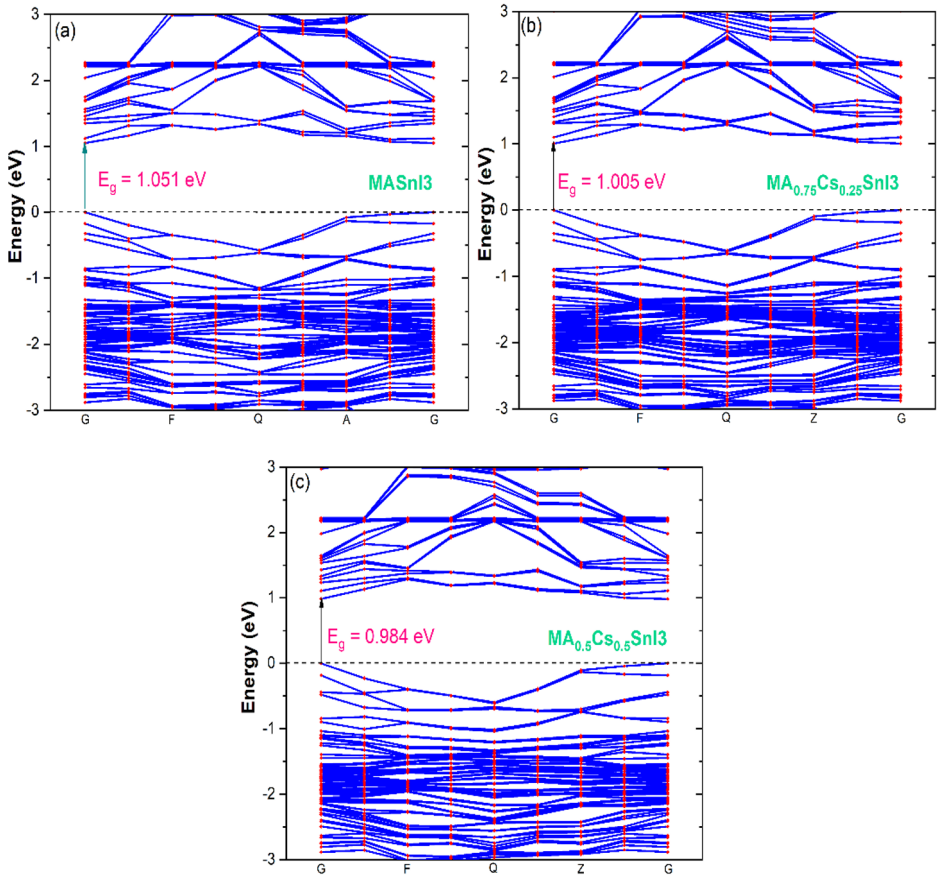

Fig. 2. Band Structures of (a) $MASnI_3$, (b) $MA_{0.75}Cs_{0.25}SnI_3$, and (c) $MA_{0.5}Cs_{0.5}SnI_3$ systems.

3.2 Optical properties

3.2.1 Absorption

In this study, we investigated the wavelength-dependent absorption coefficient in the 200–800 nm range of pristine $MASnI_3$ and Cs-doped $MASnI_3$ structures, as illustrated in Fig. 3. The spectrum of absorbing radiation for pristine $MASnI_3$ shows a peak at 394.79 nm, with a maximum absorption intensity of 70603.42 cm^{-1}. The absorption peak of $MASnI_3$ perovskite at 394.79 nm corresponds to electronic transitions within the material, specifically the excitation of electrons from the valence band to the conduction band. Since 394.79 nm lies within the visible spectrum, this peak represents the photon energy necessary to excite electrons, which strongly affects the material's optoelectronic performance. Furthermore, Cs doping in $MASnI_3$ results in a reduced absorption coefficient in the UV region while enhancing absorption in the visible range. Both pristine and Cs-doped $MASnI_3$ structures demonstrate strong light absorption across the visible spectrum, making them promising candidates for solar cell applications.

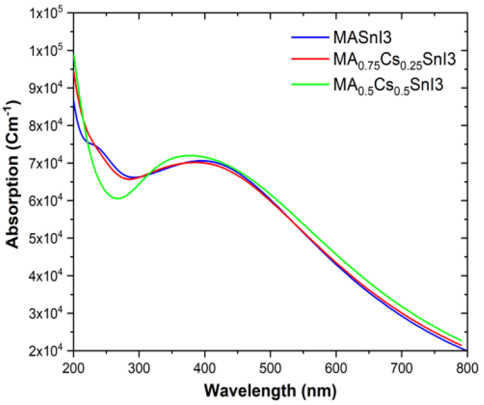

Fig. 3. Wavelength-dependent absorption coefficient for pristine $MASnI_3$, $MA_{0.75}Cs_{0.25}SnI_3$, and $MA_{0.5}Cs_{0.5}SnI_3$ structures.

3.2.2 Dielectric function

One of the most important parameters for describing the optical properties of perovskite materials is the complex dielectric function, $\varepsilon(\omega)$. It provides a detailed description of how light interacts with and propagates through these materials. This function consists of two components: The real part, $\varepsilon_1(\omega)$, which represents the material's ability to store electromagnetic energy, and the imaginary part, $\varepsilon_2(\omega)$, which corresponds to energy absorption within the material [26]:

$$\varepsilon(\omega) = \varepsilon_1(\omega) + i\varepsilon_2(\omega) \quad (1)$$

The real (ε_1) and imaginary (ε_2) parts of the dielectric function for pristine and cesium-doped $MASnI_3$ perovskites were calculated across the 200–800 nm wavelength range, as illustrated in Fig. 4. For the Cs-doped $MASnI_3$ perovskite, a reduction in the $\varepsilon_1(\omega)$ component is observed in both the UV and visible regions. This decrease is attributed to structural modifications induced by Cs doping. The smaller ionic radius of Cs^+ can lead to a more compact lattice structure, which in turn decreases the material's polarizability. This decrease

in polarizability directly affects $\varepsilon_1(\omega)$, causing it to decline. The ε_2 component, which reflects the material's absorption characteristics, shows a decrease in the UV region but an increase in the visible range. The reduction in the UV range is likely due to a fewer electronic transitions requiring higher-energy photons, while the increase in the visible range is associated with enhanced absorption of visible light. This enhancement in ε_2 in the visible range is particularly important, as it suggests that cesium doping improves the material's ability to absorb visible light, which is advantageous for optoelectronic applications. Additionally, the peaks in ε_2 for the $MASnI_3$ perovskite are linked to electronic excitations, and Cs doping intensifies these effects in the visible spectrum. The ability of both pristine and cesium-doped $MASnI_3$ to absorb a wide range of photon energies further expands the material's potential for use in various optoelectronic applications.

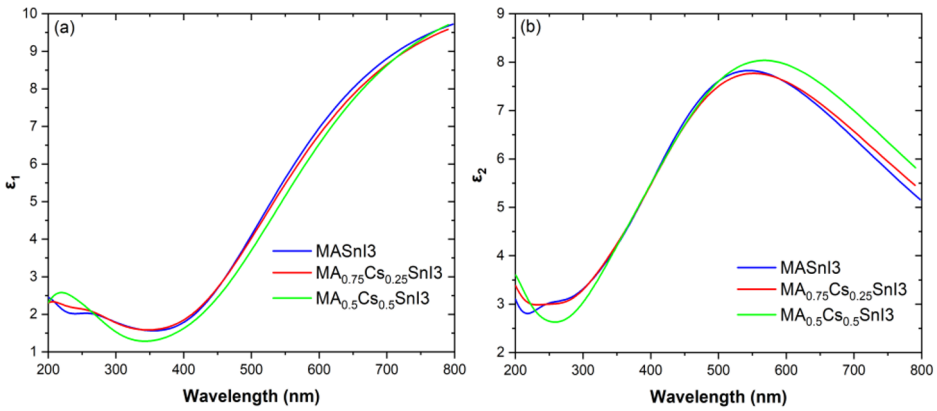

Fig. 4. Wavelength-dependent dielectric function for pristine and Cs-doped $MASnI_3$ structures.

3.2.3 Refractive index

The complex refractive index is a valuable parameter for describing how an electromagnetic wave interacts with a material as it propagates through it, relative to a vacuum. The imaginary component (k) of this refractive index accounts for the wave's attenuation or absorption within the material, the real component (n) determines the degree of refraction as it passes through the material [27]:

$$n^*(\omega) = n(\omega) + ik(\omega) \quad (2)$$

Figure 5 illustrates the wavelength-dependent variations of the real (n) and imaginary (k) components of the refractive index for pristine and Cs-doped $MASnI_3$ perovskite, as obtained from the CASTEP calculations. The incorporation of cesium as a dopant in $MASnI_3$ perovskites results in a decrease in the refractive index within the visible spectrum, implying an increase in the speed of light propagation through the $MASnI_3$ material. Moreover, the extinction coefficient (k) remains significant for both pristine and Cs-doped $MASnI_3$ in the visible region, indicating that light absorption remains substantial even after doping. A comparative analysis of the ε_2 and k components (see Fig. 4b and 5b) reveals similar trends, demonstrating a strong correlation between these parameters and their influence on the material's optical absorption properties. These results provide valuable insights into the interaction of light with pristine and cesium-doped $MASnI_3$ perovskites, offering useful information for their potential optoelectronic applications.

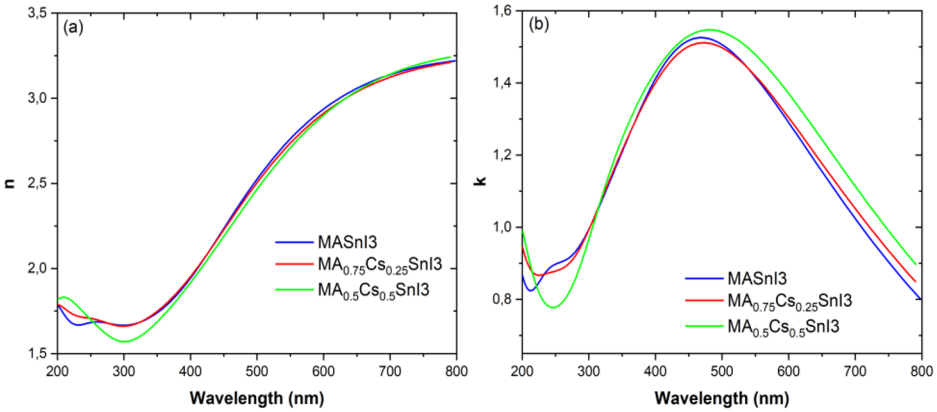

Fig. 5. Wavelength-dependent refractive index (a) and extinction coefficient (b) for pristine and Cs-doped $MASnI_3$.

3.2.4 Optical conductivity

The optical conductivity, $\sigma(\omega)$, spectrum provides insight into the material's response to incident light over a wide range of frequencies. It is a complex function that can be separated into its real (σ_1) and imaginary (σ_2) components:

$$\sigma(\omega) = \sigma_1(\omega) + i\sigma_2(\omega) \quad (3)$$

$$\sigma_1(\omega) = 2nk\left(\frac{\omega}{4\pi}\right) \quad (4)$$

$$\sigma_2(\omega) = [1 - (n^2 - k^2)]\left(\frac{\omega}{4\pi}\right) \quad (5)$$

The real (σ_1) and imaginary (σ_2) components of the optical conductivity for pristine $MASnI_3$ perovskite, as illustrated in Fig. 6, exhibit significant changes following cesium doping. In the undoped material, σ_1 exhibits a pronounced peak in the visible range, primarily due to specific electronic transitions within this region. However, upon cesium incorporation, there is a noticeable reduction in σ_1 is observed in the UV region, accompanied by an increase in the visible range. This shift can be attributed to modifications in the material's electronic transitions and band structure induced by cesium doping, which alters the density of states near the Fermi level and facilitates additional optical transitions within the visible spectrum. Regarding the imaginary part, σ_2, the pristine $MASnI_3$ shows a broad peak extending across the UV-visible range. With the introduction of cesium, the σ_2 peak becomes more pronounced, suggesting an enhancement in the intensity of interband transitions. This enhancement is likely due to increased overlap of electronic states, possibly driven by variations in crystal symmetry and lattice parameters induced by cesium incorporation. These observations highlight the influence of cesium on the optical behavior, revealing a complex interplay between structural changes and electronic behavior.

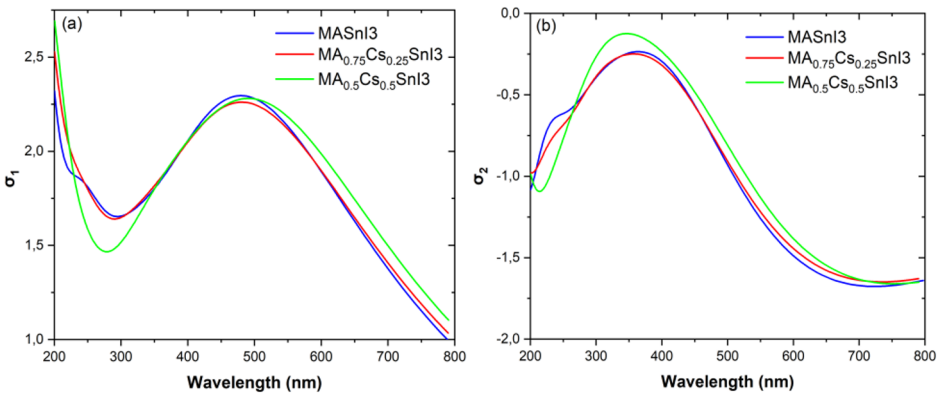

Fig. 6. Optical conductivity for pristine and Cs-doped $MASnI_3$ structures as a function of wavelength.

4 Conclusions

This study investigated the impact of cesium (Cs) doping on the optoelectronic properties of $CH_3NH_3SnI_3$ perovskite. These properties were comprehensively analyzed over a range of incident photon energies. The results revealed a consistent reduction in the band gap with increasing Cs concentration. Moreover, as Cs doping level increased, the absorption intensity in the visible region enhanced, while it decreased in the UV range, highlighting the potential of Cs-doped $MASnI_3$ perovskite for solar cell applications. In addition, the optical conductivity increased with higher Cs doping, indicating enhanced electrical conduction under light irradiation. Overall, the optoelectronic and optical characteristics of $MASnI_3$ perovskite suggest that it is a promising material for photovoltaic applications.

Acknowledgement

The authors express their sincere gratitude to everyone who contributed to this research, with special thanks to Sultan Moulay Slimane University and the Africa Graphene Center.

Funding: No funding available for the proposed research.

Data availability statement: No datasets were generated or analysed during the current study.

Author contributions

The authors declare that they have no financial interests or personal relationships that could have influenced the work presented in this paper.

References

1. A. Shukla, V.K. Sharma, S.K. Gupta, A.S. Verma, Computational determination of the physical-thermoelectric parameters of tin-based organomatallic halide perovskites (CH3NH3SnX3, X = Br and I): Emerging materials for optoelectronic devices. Materials Chemistry and Physics. **253**, 123389 (2020). https://doi.org/10.1016/j.matchemphys.2020.123389
2. K. Hossain, S. Khanom, F. Israt, M.K. Hossain, M.A. Hossain, F. Ahmed, First-principles study on structural, mechanical and optoelectronic properties of lead-free

mixed Ge–Sn hybrid organic-inorganic perovskites. Solid State Communications. **320**, 114024 (2020). https://doi.org/10.1016/j.ssc.2020.114024

3. Y.Q. Huang, J. Su, Q.F. Li, D. Wang, L.H. Xu, Y. Bai, Structure, optical and electrical properties of CH3NH3SnI3 single crystal. Physica B: Condensed Matter. **563**, 107–112 (2019). https://doi.org/10.1016/j.physb.2019.03.035
4. S.S. Bagade, M.M. Malik, P.K. Patel, The charm of entwining two major competitors CZTS & CH3NH3SnI3 to feasibly explore photovoltaic world beyond Shockley–Queisser limit. Surfaces and Interfaces. **46**, 104020 (2024). https://doi.org/10.1016/j.surfin.2024.104020
5. K. Yan, B. Sun, T. Lu, X.D. Feng, Simulation of MASnI3-based inverted perovskite solar cells with double hole transport layers and an electron transport layer. Optik. **287**, 171100 (2023). https://doi.org/10.1016/j.ijleo.2023.171100
6. A. Najim, L. Moulaoui, A. Laassouli, O. Bajjou, K. Rahmani, Design and simulation of an organic–inorganic GO/P3HT/MASnI3 solar cell using the SCAPS-1D program. Electr Eng. **107**, 7657–7671 (2025). https://doi.org/10.1007/s00202-024-02941-4
7. M.F. Rahman, M.M. Tasdid, M.M. Fadhali, M. Sharma, M. Akermi, Unlocking Cesium based new double absorber perovskite solar cells with efficiency above 28% for next generation solar cell. Photonics and Nanostructures - Fundamentals and Applications. **64**, 101371 (2025). https://doi.org/10.1016/j.photonics.2025.101371
8. A. Najim, A. Bakour, O. Bajjou, Y. Chrafih, K. Rahmani, Electronic and optical properties of C60 under the influence of alkali metal injection: A DFT study. Struct Chem. **36**, 887–900 (2025). https://doi.org/10.1007/s11224-024-02417-y
9. M. Tarekuzzaman, M.S. Parves, M.Z. Rahman, S.S. Hasan, Cesium-Based Perovskite Hydrides: A Theoretical Insight into Hydrogen Storage and Optoelectronic Characteristics. Solid State Communications. **404**, 116043 (2025). https://doi.org/10.1016/j.ssc.2025.116043
10. A. Ahmad, S.T. Jan, H.A. Khan, M. Sheraz, W.U.K. Tareen, T.C. Chuah, I.E. Lee, H. Ali, Compatibility analysis of novel inorganic cesium perovskites with emerging charge transport layers through design optimization. Energy Nexus. **17**, 100400 (2025). https://doi.org/10.1016/j.nexus.2025.100400
11. J.H. Yoo, S.B. Kwon, J. Park, S.H. Choi, H.C. Yoo, B.K. Kang, Y.H. Song, S. Hong, D.H. Yoon, Potential usage of cesium manganese halide for multi-functional optoelectronic devices: Display & photodetector application. Chemical Engineering Journal. **479**, 147277 (2024). https://doi.org/10.1016/j.cej.2023.147277
12. Z.Q. Ma, H. Pan, P.K. Wong, A first-principles study on the structural and electronic properties of Sn-based organic–inorganic halide perovskites. J. Electron. Mater. **45**, 5956–5966 (2016). https://doi.org/10.1007/s11664-016-4822-9
13. R. Batool, T. Mahmood, S. Mahmood, A.A. Bhatti, A computational study of alkali (Na, K, Cs) doped methylammonium lead iodide perovskite. Physica B. **672**, 415469 (2024). https://doi.org/10.1016/j.physb.2023.415469
14. G. Niu, W. Li, J. Li, X. Liang, L. Wang, Enhancement of thermal stability for perovskite solar cells through cesium doping. RSC advances. **7**, 17473-17479 (2017). https://doi.org/10.1039/C6RA28501E
15. L. Moulaoui, A. Najim, A. Laassouli, O. Bajjou, A. Bakour, Y. Lachtioui, K. Rahmani, B. Manaut, Maximizing the performance of FTO/GO/FASnI3/Cu solar cells: Advanced analysis using SCAPS-1D achieving an efficiency of 20.63%. Results in Optics. (2025). https://doi.org/10.1016/j.rio.2025.100869

16. H. Choi, J. Jeong, H.B. Kim, S. Kim, B. Walker, G.H. Kim, J.Y. Kim, Cesium-doped methylammonium lead iodide perovskite light absorber for hybrid solar cells. Nano Energy. **7**, 80–85 (2014). http://dx.doi.org/10.1016/j.nanoen.2014.04.017
17. H. Arif, M.B. Tahir, M. Sagir, H. Alrobei, M. Alzaid, S. Ullah, M. Hussien, Effect of potassium on the structural, electronic, and optical properties of CsSrF3 fluro perovskite: First-principles computation with GGA-PBE. Optik. **259**, 168741 (2022). https://doi.org/10.1016/j.ijleo.2022.168741
18. A. Taya, P. Rani, J. Thakur, M.K. Kashyap, First principles study of structural, electronic and optical properties of Csdoped CH3NH3PbI3 for photovoltaic applications. Vacuum. **160**, 440–444 (2019). https://doi.org/10.1016/j.vacuum.2018.12.008
19. S. Chen, T. Bimenyimana, M. Guli, First-principles study on the electronic properties of perovskites MASnaPb (1− a) XbY (3− b)(X, Y= Cl, Br, I). Results in Physics. **14**, 102408 (2019). https://doi.org/10.1016/j.rinp.2019.102408
20. L. Peng, W. Xie, Theoretical and experimental investigations on the bulk photovoltaic effect in lead-free perovskites MASnI3 and FASnI3. RSC Adv. **10**, 14679 (2020). https://doi.10.1039/D0RA02584D
21. S. Bouhmaidi, A. Marjaoui, A. Talbi, M. Zanouni, K. Nouneh, L. Setti, A DFT study of electronic, optical and thermoelectric properties of Ge-halide perovskites CsGeX3 (X=F, Cl and Br). Computational Condensed Matter. **31**, e00663 (2022). https://doi.org/10.1016/j.cocom.2022.e00663
22. A. Najim, O. Bajjou, A. Bakour, Y. Chrafih, K. Rahmani, A theoretical approach on using the electric field to control the band structures and optical properties of fullerene. MRS Advances. **9**, 1448–1453 (2024). https://doi.org/10.1557/s43580-024-00935-9
23. M.M. Islam, M.M. Hasan, M.R. Islam, S. Ahmad, DFT insights into the pressure-induced ultraviolet to visible band gap engineering of TlMgF3 cubic halide perovskites for optoelectronic applications. Journal of Physics and Chemistry of Solids. **191**, 112037 (2024). https://doi.org/10.1016/j.jpcs.2024.112037
24. A. Najim, O. Bajjou, A. Bakour, M. Boulghallat, K. Rahmani, A fundamental study on the electronic and optical properties of graphene oxide under an external electric field. Mod. Phys. Lett. B. **38**, 1–21 (2024). https://doi.org/10.1142/S0217984924500325
25. R. Sabetvand, M.E. Ghazi, M. Izadifard, DFT study of electronic and optical properties of CH3NH3SnI3 perovskite. Energy Sources, Part A: Recovery, Utilization, and Environmental Effects. (2020). https://doi.org/10.1080/15567036.2020.1805047
26. L. Moulaoui, A. Najim, M. Archi, M. Al-Hattab, O. Bajjou, A. Bakour, Y. Lachtioui, K. Rahmani, B. Manaut, Theoretical study of the Sb-substitution effect on the optoelectronic properties of Cs2AgBiBr6 double perovskite. Results in Chemistry. **13**, 102025 (2025). https://doi.org/10.1016/j.rechem.2025.102025
27. A. Dey, R. Sharma, S.A. Dar, I.H. Wani, Cubic PbGeO3 perovskite oxide: A compound with striking electronic, thermoelectric and optical properties, explored using DFT studies. Computational Condensed Matter. **26**, e00532 (2021). https://doi.org/10.1016/j.cocom.2020.e00532